

SCIENTIFIC REPORTS

OPEN

Identifying influential spreaders by gravity model

Zhe Li¹, Tao Ren¹, Xiaoqi Ma², Simiao Liu¹, Yixin Zhang¹ & Tao Zhou³

Identifying influential spreaders in complex networks is crucial in understanding, controlling and accelerating spreading processes for diseases, information, innovations, behaviors, and so on. Inspired by the gravity law, we propose a gravity model that utilizes both neighborhood information and path information to measure a node's importance in spreading dynamics. In order to reduce the accumulated errors caused by interactions at distance and to lower the computational complexity, a local version of the gravity model is further proposed by introducing a truncation radius. Empirical analyses of the Susceptible-Infected-Recovered (SIR) spreading dynamics on fourteen real networks show that the gravity model and the local gravity model perform very competitively in comparison with well-known state-of-the-art methods. For the local gravity model, the empirical results suggest an approximately linear relation between the optimal truncation radius and the average distance of the network.

Network science is playing an increasingly significant role in many domains including physics, sociology, engineering, biology, management, and so on¹. The heterogeneous nature of real networks² asks for a crucial question: How to quantitatively measure a node's importance in a dynamical process? Taking spreading dynamics as an example, a popular star in Twitter may remarkably accelerate a rumor and a few superspreaders could largely expand the epidemic prevalence of a disease³. Therefore, a good answer to the above question, namely an efficient algorithm to identify influential spreaders in complex networks, can help to better control the outbreak of an epidemic⁴, optimize the use of limited resources to facilitate the dissemination of information⁵, prevent catastrophic disruptions of power grid or the Internet⁶, discover the candidates of drug target and essential proteins⁷, and so on. Till far, most known methods only make use of the structural information⁸, which can be roughly classified into neighborhood-based centralities and path-based centralities.

Typical representatives of the neighborhood-based centralities are degree centrality⁹ (DC), H-index¹⁰ and *k*-shell decomposition method¹¹ (KS). For DC, nodes with larger degrees are more influential. For H-index, nodes connecting with many large-degree neighbors are more influential. KS assigns a *k*-shell index to each node based on its topological location, where nodes closer to the core of the network will get higher *k*-shell indices, and nodes in the periphery will get lower *k*-shell indices. The nodes with higher *k*-shell indices are considered to be more influential. Besides, PageRank¹² and LeaderRank¹³ are two representative neighborhood-based iterative methods, both suggesting that the influence of a node is determined by the influences of its neighbors. Two well-studied path-based centralities are closeness centrality¹⁴ (CC) and betweenness centrality¹⁵ (BC). CC claims that a node averagely closer to other nodes is more influential while BC assumes that a node locating in many shortest paths is of high influence.

Inspired by the gravity law, recently, Ma *et al.*¹⁶ proposed two gravity-law-based algorithms by considering both neighborhood information and path information (see Methods for the details of algorithms). Analogously, we proposed a variant algorithm named gravity model (GM), which also takes into account both neighborhood information and path information, where a node with larger degrees (neighborhood information) and averagely shorter distances to other nodes (path information) is more influential. Furthermore, we propose a local version of the gravity model (named as local gravity model, LGM for short) to lower the computational complexity and reduce the possible noise caused by interactions at distance. Such local model only accounts for pairwise interactions within a truncation radius. Empirical results show that GM and LGM perform very competitively in comparison with well-known state-of-the-art methods. In particular, for LGM, an empirically linear relation between the optimal truncation radius and the average distance of the network is observed.

¹Software College, Northeastern University of China, Shenyang, 110819, P.R. China. ²School of Science and Technology, Nottingham Trent University, Nottingham, NG11 8NS, United Kingdom. ³Complex Lab, University of Electronic Science and Technology of China, Chengdu, 611731, P.R. China. Correspondence and requests for materials should be addressed to T.R. (email: chinarentao@163.com) or T.Z. (email: zhutou@ustc.edu)

Networks	N	E	$\langle k \rangle$	$\langle d \rangle$	C	r	H	β_c
Jazz	198	2472	27.6970	2.2350	0.6334	0.0202	1.3951	0.0266
NS	379	914	4.8232	6.0419	0.7981	-0.0817	1.6630	0.1424
GrQc	4158	13422	6.4560	6.0494	0.6648	0.6392	2.7852	0.0589
EEC	986	16064	32.5842	2.5869	0.4505	-0.0257	2.2912	0.0136
Email	1133	5451	9.6222	3.6060	0.2540	0.0782	1.9421	0.0565
PG	6299	20776	6.5966	4.6430	0.0150	0.0355	2.6764	0.0600
Enron	33696	180811	10.7319	4.0252	0.7081	-0.1165	13.2655	0.0071
PB	1222	16714	27.3552	2.7375	0.3600	-0.2213	2.9707	0.0125
Facebook	4039	88234	43.6910	3.6925	0.6170	0.0636	2.4392	0.0095
WV	7066	100736	28.5129	3.2475	0.2090	-0.0833	5.0992	0.0069
Sex	15810	38540	4.8754	5.7846	0	-0.1145	5.8276	0.0365
USAir	332	2126	12.8072	2.7381	0.7494	-0.2079	3.4639	0.0231
Power	4941	6594	2.6691	18.9892	0.1065	0.0035	1.4504	0.3483
Router	5022	6258	2.4922	6.4488	0.0329	-0.1384	5.5031	0.0786

Table 1. The basic topological features of the fourteen real networks. N and E are the number of nodes and links. $\langle k \rangle$ and $\langle d \rangle$ are the average degree and the average distance. C and r are the clustering coefficient and the assortative coefficient. H is the degree heterogeneity. β_c is the epidemic threshold of the SIR model.

Results

Algorithms. Individually speaking, nodes with large degrees are likely to be more influential. In addition, a node is of higher impacts on nearby nodes¹⁷. According to the above issues and inspired by the gravity law, we regard the degree of a node as its mass, and the shortest distance between two nodes as their distance. Hence a node i 's influence can be estimated as

$$S(i) = \sum_{j \neq i} \frac{k_i k_j}{d_{ij}^2}, \quad (1)$$

where k_i is the degree of node i , d_{ij} is the shortest distance between node i and node j , and j runs over all nodes other than i . Obviously, a node with many neighbors and be close to most nodes is more influential according to Eq. 1. Such method is named as gravity model as it adopts the formula of the gravity law.

Although GM can identify the nodes averagely closer to other nodes and with larger degrees, it has two shortcomings. Firstly, to calculate shortest distances between all node pairs is time-consuming for large-scale networks¹⁸. Secondly, in real propagation a node is hard to impact other nodes at distance and to estimate the interacting strength between distant nodes is usually inaccurate since the step-by-step decaying influence will be disturbed by accumulated noise¹⁹. Therefore, by introducing a truncation radius, we only consider the pairwise interactions within the truncation radius. Hence a node i 's influence can be estimated as

$$S_R(i) = \sum_{d_{ij} \leq R, j \neq i} \frac{k_i k_j}{d_{ij}^2}, \quad (2)$$

where R is the truncation radius. Such method (Eq. 2) is named as local gravity model as it only takes into account local information of the network.

Data description. In this paper, fourteen real networks from disparate fields are used to test the performance of GM and LGM, including three collaboration networks (Jazz, NS and GrQc), four communication networks (EEC, Email, PG and Enron), four social networks (PB, Facebook, WV and Sex), one transportation network (USAir), one infrastructure network (Power) and one technological network (Router). Jazz²⁰ is a collaboration network of jazz musicians. NS²¹ is a co-authorship network of scientists working on network science. GrQc²² is a collaboration network of eprint articles in arXiv categories General Relativity and Quantum Cosmology. EEC²³ describes email interchanges between institution members of a large European research institution. Email²⁴ describes email interchanges between users including faculty, researchers, technicians, managers, administrators, and graduate students of the Rovira i Virgili University. PG²² is a snapshot of the Gnutella peer-to-peer file sharing network from August 2002. Enron²⁵ is the Enron email network. PB²⁶ is a network of US political blogs. Facebook²⁷ describes social circles from Facebook. WV²⁸ is a network of Wikipedia who-votes-on-whom. Sex²⁹ is a bipartite network in which nodes are females (sex sellers) and males (sex buyers) and links between them are established when males write posts indicating sexual encounters with females. USAir³⁰ is the US air transportation network. Power³¹ is the power grid of the western United States. Router³² is a symmetrized snapshot of the structure of the Internet at the level of autonomous systems. These networks' topological features (including the number of nodes, the number of links, the average degree, the average distance, the clustering coefficient³¹, the assortative coefficient³³, the degree heterogeneity³⁴ and the epidemic threshold³⁵ of the SIR model³⁶) are shown in Table 1.

Networks	BC	CC	DC	H-index	KS	G	G+	GM	LGM
Jazz	0.4590	0.7043	0.8088	0.8417	0.7608	0.8677	0.9025	0.8533	0.8634
NS	0.2979	0.3415	0.5728	0.5561	0.5051	0.8110	0.8464	0.7611	0.8231
GrQc	0.3231	0.5464	0.6443	0.6362	0.6115	0.8337	0.7922	0.7684	0.8417
EEC	0.7151	0.8610	0.8468	0.8641	0.8525	0.8943	0.9189	0.8803	0.9022
Email	0.6254	0.8104	0.7665	0.7887	0.7707	0.8720	0.9076	0.8265	0.8671
PG	0.5605	0.6916	0.5941	0.6216	0.5897	0.6992	0.7082	0.6632	0.6900
Enron	0.3387	0.4241	0.4657	0.4654	0.4636	0.4859	0.4610	0.5055	0.5075
PB	0.6839	0.7865	0.8580	0.8732	0.8633	0.9001	0.9211	0.8887	0.9067
Facebook	0.4450	0.3362	0.6704	0.6948	0.6965	0.7117	0.7361	0.7160	0.7394
WV	0.6305	0.6748	0.6763	0.6788	0.6778	0.6919	0.6917	0.6895	0.6926
Sex	0.4251	0.6119	0.4774	0.4889	0.4934	0.6606	0.6386	0.6092	0.6713
USAir	0.5181	0.8052	0.7320	0.7525	0.7470	0.8514	0.9012	0.8286	0.8817
Power	0.3205	0.3653	0.4207	0.3935	0.3084	0.6610	0.7544	0.6128	0.6947
Router	0.3059	0.5120	0.3107	0.1917	0.1791	0.6216	0.6226	0.5782	0.6441

Table 2. The algorithms' accuracies for $\beta = \beta_c$, measured by the Kendall's Tau (τ). The best performed algorithm for each network is emphasized by bold.

Empirical results. We apply the well-known SIR model³⁶ to compare the rankings of influences produced by algorithms and simulations. Initially, one node (called seed) in the network is in the infected state (I) and the others are in the susceptible state (S). Each of the infected nodes can infect its susceptible neighbors with probability β . And in each step, every infected node changes to be recovered and will never participate in the dynamics with probability λ . The spreading process repeats until there are no more infected nodes in the network. The influence of any node i can be estimated by

$$F(i) = N_r/N, \quad (3)$$

where N_r is the number of recovered nodes at the end of the dynamics. For simplicity, we set $\lambda = 1$, and the corresponding epidemic threshold³⁴ is

$$\beta_c \approx \frac{\langle k \rangle}{\langle k^2 \rangle - \langle k \rangle}, \quad (4)$$

where $\langle k \rangle$ and $\langle k^2 \rangle$ denote the average degree and the second-order moment of the degree distribution.

Given a network and the transmission probability β , to obtain the standard ranking of nodes' influences, we implement 1000 independent runs, in each run every node is selected once as the seed once. The accuracy of an algorithm is measured by the Kendall's Tau (τ)³⁷ between the standard ranking and the ranking by the algorithm (see details in Methods). A larger value of τ means a stronger correlation between the two sequences and thus a better performance. Table 2 compares the accuracies of the two proposed algorithms (i.e., GM and LGM) and seven benchmark algorithms (see details about the benchmark algorithms in Methods). The transmission probability for each case is fixed as $\beta = \beta_c$ (for more values of β , see Fig. 1) and the parameters in relevant algorithms are all adjusted to their optimal values subject to the largest τ .

As shown in Table 2, both GM and LGM are very competitive. In particular, G+ and LGM perform best among the nine algorithms. Notice that, G+ also adopts the gravity formula¹⁶ (see Methods) but a node's mass in G+ is defined as its k -shell index so G+ is indeed a global index. The results reported in Table 2 demonstrate the advantage of gravity models (e.g., G, G+, GM, LGM) and show that a local index (LGM) can outperform most benchmark algorithms including some global indices. As shown in Fig. 1, results for other values of β not too far from the threshold are consistent to the one at β_c , suggesting the robustness of our findings.

Since to determine the optimal truncation radius, denoted by R^* , asks for more computation, we want to see whether topological information can be used to profile R^* . As shown in Fig. 2, R^* approximately scales linearly with the average distance, as

$$R^* \approx \frac{1}{2} \langle d \rangle \quad (5)$$

at $\beta = \beta_c$. Such approximately linear relation also holds for other values of β not so far from β_c . This empirical relation can save computational cost in practice.

Discussion

To measure influences of nodes in a certain networked dynamics, a straightforward method is to estimate the interacting strengths between node pairs in advance. The gravity law is a simple, elegant and representative formula that estimates the interacting strength between two nodes by simultaneously considering the intrinsic influences of the two nodes themselves and the distance between them. In this paper, the gravity model (Eq. 1) makes use of both the neighborhood information and the path information, which were separately adopted in many previous methods. Furthermore, to reduce the computational complexity and to avoid the accumulated noises

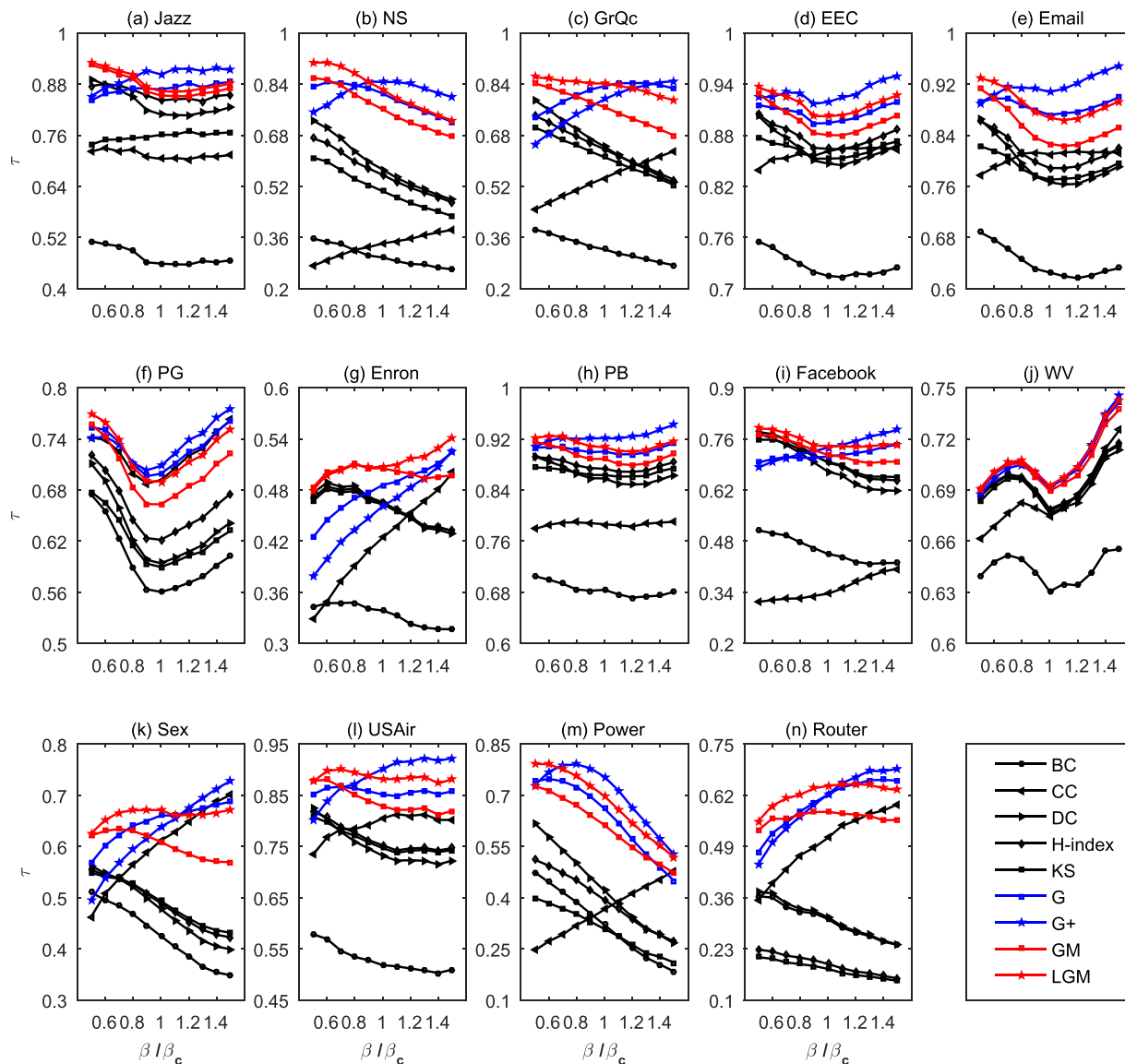


Figure 1. The algorithms' accuracies for different β , measured by the Kendall's Tau (τ).

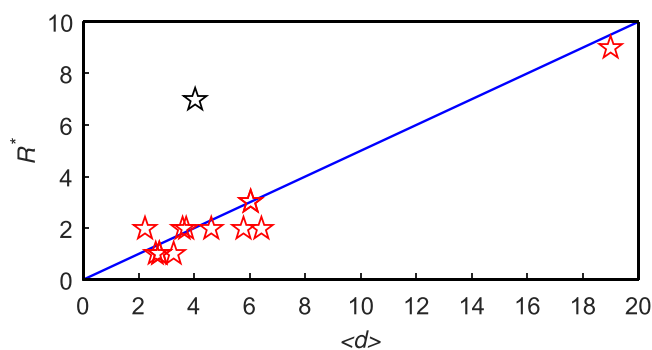


Figure 2. The relation between R^* and $\langle d \rangle$ for $\beta = \beta_c$. Fourteen pentagrams represent fourteen networks and the slope of the blue line is $1/2$. The pentagram in black is the outlier – the Enron network. Although the optimal truncation radius $R^* = 7$ is much different from what Eq. 5 predicts (i.e., $R = 2$), the algorithmic accuracy at $R = 2$ ($\tau = 0.4949$) is very close to the best accuracy at $R^* = 7$ ($\tau = 0.5075$) in comparison with the traditional methods (e.g., about 0.34 for BC, 0.42 for CC and 0.46 for DC, KS and H-index). That is to say, to apply Eq. 5 can still achieve much better algorithmic performance than the traditional methods.

Networks	$R=1$	$R=2$	$R=3$	$R=4$	$R=5$
Jazz	0.9748	0.9927	0.9976	0.9981	0.9993
NS	0.9348	0.9629	0.9752	0.9797	0.9829
GrQc	0.9197	0.9161	0.9380	0.9628	0.9721
EEC	0.9773	0.9882	0.9963	0.9978	0.9988
Email	0.9596	0.9770	0.9840	0.9927	0.9963
PG	0.9413	0.9596	0.9766	0.9886	0.9957
Enron	0.8479	0.8958	0.9274	0.9611	0.9793
PB	0.9682	0.9865	0.9956	0.9977	0.9984
Facebook	0.8797	0.9431	0.9768	0.9842	0.9899
WV	0.9668	0.9760	0.9958	0.9982	0.9989
Sex	0.9039	0.9042	0.9500	0.9615	0.9712
USAir	0.9607	0.9697	0.9858	0.9912	0.9939
Power	0.9486	0.9672	0.9717	0.9754	0.9785
Router	0.8416	0.9007	0.9402	0.9600	0.9720

Table 3. The Kendall's Tau between two rankings of nodes' influences produced by the LGM with truncation radius R and $R+1$.

through long paths, we proposed a local version of the gravity model (LGM, see Eq. 2). Both GM and LGM are very competitive, and of particular interests, the LGM requires less computation yet performs even better. Indeed, LGM is one of the two best-performed methods among many well-known benchmark algorithms.

A potential disadvantage of LGM is that it has a free parameter, namely the truncation radius R . The negative effects of the existence of R are twofold. Firstly, it asks for more computation to determine the optimal value of R . Secondly, if the optimal value, say R^* , is very large, the computational complexity of LGM will be more or less the same to GM. Fortunately, as shown in Fig. 2, we found an empirical relation between R^* and the average distance $\langle d \rangle$, so that if the computational resource is highly limited, we can use the relation (see Eq. 5) to approximate R^* . In addition, since most real networks are of small-world property^{31,38}, R^* should be small and thus it requires much less computation than GM. Fortunately, the difference between two rankings of nodes produced by neighboring R will quickly converge to a very small value, so that to choose a small value of R will probably perform very well. In Table 3, we show the values of $\tau(R)$, which is the Kendall's tau between two rankings of nodes' influences with truncation radius being R and $R+1$. One can observe that after $R=5$, all networks are of $\tau(R) > 0.97$ and a half of them are of $\tau(R) > 0.99$. This indicates a strong saturation, namely the increasing of R will produce almost the same rankings if the value of R is already large.

Another similar model (named G+, see Eq. 11) shows very close performance to LGM. In comparison, LGM is more efficient since it completely depends on the local topological structure and thus can be calculated not only faster but also under the case where the global topology is not known. In the absence of global topology, G+ cannot be obtained since it sets a node's k -shell index as its mass, and to determine the k -shell index needs the knowledge of the whole network. In despite the difference between G+ and LGM, the very good performance of G+ and LGM strongly suggest the validity and advantage of the usage of the gravity law to estimate the interacting strength. Of course, both G+ and LGM are very simple and general, which can be further improved by the following aspects (also leaving as open issues for future studies). Firstly, by introducing a few tunable parameters that can adjust the relative importance of mass and distance (e.g., to replace d^2 by some d^a and/or to replace k by some k^b) may result in more accurate predictions as indicated by known variants of the gravity law in other applications³⁹. Secondly, we should explore how the topological features and dynamical processes affect the prediction accuracy and thus improve the original methods by introducing some topology-dependent and/or dynamics-sensitivity items^{40,41}. Thirdly, the original gravity law is symmetric, while due to the different roles of different nodes or the essentially asymmetric nature of the dynamics^{42,43}, the influence from node i onto node j could be different from the influence from node j onto node i , where an asymmetric form of the gravity law may be relevant.

Methods

The Kendall's Tau. The Kendall's Tau³⁷ is an index measuring the correlation strength between two sequences. Considering two sequences with N elements, $X = (x_1, x_2, \dots, x_N)$ and $Y = (y_1, y_2, \dots, y_N)$. Any pair of two-tuples (x_i, y_i) and (x_j, y_j) ($i \neq j$) are concordant if both $x_i > x_j$ and $y_i > y_j$, or both $x_i < x_j$ and $y_i < y_j$. They are discordant if $x_i > x_j$ and $y_i < y_j$ or $x_i < x_j$ and $y_i > y_j$. If $x_i = x_j$ or $y_i = y_j$, the pair is neither concordant nor discordant. The Kendall's Tau of two sequences X and Y can be calculated as

$$\tau = \frac{2(n_+ - n_-)}{N(N-1)}, \quad (6)$$

where n_+ and n_- denote the number of concordant and discordant pairs, respectively. It can be seen that the extent to which τ exceeds zero indicates the strength of the correlation.

Benchmark centralities. Degree Centrality⁹ of node i is defined as

$$DC(i) = \sum_j a_{ij}, \quad (7)$$

where $A = \{a_{ij}\}$ is the adjacency matrix, that is, $a_{ij} = 1$ if i and j are connected and 0 otherwise.

H-index¹⁰ of node i , denoted by $H(i)$, is defined as the maximal integer satisfying that there are at least $H(i)$ neighbors of node i whose degrees are all no less than $H(i)$. Such index is an extension of the famous H-index in scientific evaluation⁴⁴ to network analysis.

Closeness Centrality¹⁴ of node i is defined as

$$CC(i) = \frac{N - 1}{\sum_{j \neq i} d_{ij}}. \quad (8)$$

Betweenness Centrality¹⁵ of node i is defined as

$$BC(i) = \sum_{s \neq i, s \neq t, i \neq t} \frac{g_{st}(i)}{g_{st}}, \quad (9)$$

where g_{st} is the number of shortest paths between nodes s and t , and $g_{st}(i)$ is the number of shortest paths between nodes s and t that pass through node i .

Gravity Centrality¹⁶ (G) of node i is defined as

$$G(i) = \sum_{j \in \psi_i} \frac{k_s(i)k_s(j)}{d_{ij}^2}, \quad (10)$$

where $k_s(i)$ is the k -shell index of node i , and ψ_i is the set of nodes whose distance to node i is less than or equal to 3.

Extended Gravity Centrality¹⁶ ($G+$) of node i is defined as

$$G_+(i) = \sum_{j \in \Lambda_i} G(j), \quad (11)$$

where Λ_i is the set of neighbors of node i .

Data Availability

All relevant data are available at <https://github.com/MLIF/Network-Data>.

References

- Newman, M. E. J. *Networks* (Oxford University Press, Oxford, 2018).
- Caldarelli, G. *Scale-Free Networks: Complex Webs in Nature and Technology* (Oxford University Press, Oxford, 2007).
- Lloyd-Smith, J. O., Schreiber, S. J., Kopp, P. E. & Getz, W. M. Superspreading and the effect of individual variation on disease emergence. *Nature* **438**, 355–359 (2005).
- Pastor-Satorras, R. & Vespignani, A. Immunization of complex networks. *Phys. Rev. E* **65**, 036104 (2002).
- Morone, F. & Makse, H. A. Influence maximization in complex networks through optimal percolation. *Nature* **524**, 65–68 (2015).
- Albert, R., Albert, I. & Nakarado, G. L. Structural vulnerability of the North American power grid. *Phys. Rev. E* **69**, 025103 (2004).
- Csermely, P., Korcsmáros, T., Kiss, H. J., London, G. & Nussinov, R. Structure and dynamics of molecular networks: a novel paradigm of drug discovery: a comprehensive review. *Pharmacol. Ther.* **138**, 333–408 (2013).
- Lü, L. *et al.* Vital nodes identification in complex networks. *Phys. Rep.* **650**, 1–63 (2016).
- Bonacich, P. Factoring and weighting approaches to status scores and clique identification. *Math. Sociol.* **2**, 113–120 (1972).
- Lü, L., Zhou, T., Zhang, Q. M. & Stanley, H. E. The H-index of a network node and its relation to degree and coreness. *Nat. Commun.* **7**, 10168 (2016).
- Kitsak, M. *et al.* Identification of influential spreaders in complex networks. *Nat. Phys.* **6**, 888–893 (2010).
- Brin, S. & Page, L. The anatomy of a large-scale hypertextual web search engine. *Comput. Netw. ISDN Syst.* **30**, 107–117 (1998).
- Lü, L., Zhang, Y. C., Yeung, C. H. & Zhou, T. Leaders in social networks, the delicious case. *PLoS One* **6**, e21202 (2011).
- Freeman, L. C. Centrality in social networks conceptual clarification. *Soc. Networks* **1**, 215–239 (1979).
- Freeman, L. C. A set of measures of centrality based on betweenness. *Sociometry* **40**, 35–41 (1977).
- Ma, L. L., Ma, C., Zhang, H. F. & Wang, B. H. Identifying influential spreaders in complex networks based on gravity formula. *Physica A* **451**, 205–212 (2015).
- Christakis, N. A. & Fowler, J. H. The spread of obesity in a large social network over 32 years. *N. Engl. J. Med.* **357**, 370–379 (2007).
- Floyd, R. W. Algorithm 97: shortest path. *Commun. ACM* **5**, 345 (1962).
- Chen, D., Lü, L., Shang, M. S., Zhang, Y. C. & Zhou, T. Identifying influential nodes in complex networks. *Physica A* **391**, 1777–1787 (2012).
- Gleiser, P. & Danon, L. Community structure in Jazz. *Adv. Complex Syst.* **6**, 565 (2003).
- Newman, M. E. J. Finding community structure in networks using the eigenvectors of matrices. *Phys. Rev. E* **74**, 036104 (2006).
- Leskovec, J., Kleinberg, J. & Faloutsos, C. Graph evolution: densification and shrinking diameters. *ACM Trans. Knowl. Discov. Data* **1**, 2 (2007).
- Yin, H., Austin, R., Benson, J. L. & David, F. G. Local higher-order graph clustering. In *Proceedings of the 23rd ACM SIGKDD International Conference on Knowledge Discovery and Data Mining*. 555–564 (ACM Press, 2017).
- Guimerà, R., Danon, L., Díaz-Guilera, A., Giralt, F. & Arenas, A. Self-similar community structure in a network of human interactions. *Phys. Rev. E* **68**, 065103 (2003).
- Leskovec, J., Lang, K. J., Dasgupta, A. & Mahoney, M. W. Community structure in large networks: natural cluster sizes and the absence of large well-defined clusters. *Internet Math.* **6**, 29–123 (2009).
- Adamic, L. A. & Glance, N. The political blogosphere and the 2004 U.S. election: divided they blog. In *Proceedings of the 3rd international workshop on Link discovery*. 36–43 (ACM Press, 2005).
- Mcauley, J. J. & Leskovec, J. Learning to discover social circles in ego networks. *Adv. Neural Inf. Process. Syst.* **25**, 548–556 (2012).

28. Leskovec, J., Huttenlocher, D. & Kleinberg, J. Predicting positive and negative links in online social networks. In *Proceedings of the 19th international conference on World Wide Web*. 641–650 (ACM Press, 2010).
29. Rocha, L. E., Liljeros, F. & Holme, P. Simulated epidemics in an empirical spatiotemporal network of 50,185 sexual contacts. *PLoS Comput. Biol.* **7**, e1001109 (2011).
30. Batageli, V. & Mrvar, A. Pajek Datasets. Available at, <http://vlado.fmf.uni-lj.si/pub/networks/data/> (2007).
31. Watts, D. J. & Strogatz, S. H. Collective dynamics of 'small-world' networks. *Nature* **393**, 440–442 (1998).
32. Spring, N., Mahajan, R., Wetherall, D. & Anderson, T. Measuring ISP topologies with rocketfuel. *IEEE/ACM Trans. Networking* **12**, 2–16 (2004).
33. Newman, M. E. J. Assortative mixing in networks. *Phys. Rev. Lett.* **89**, 208701 (2002).
34. Hu, H. B. & Wang, X. F. Unified index to quantifying heterogeneity of complex networks. *Physica A* **387**, 3769–3780 (2008).
35. Castellano, C. & Pastor-Satorras, R. Thresholds for epidemic spreading in networks. *Phys. Rev. Lett.* **105**, 218701 (2010).
36. Hethcote, H. W. The mathematics of infectious diseases. *SIAM Rev.* **42**, 599–653 (2009).
37. Kendall, M. A new measure of rank correlation. *Biometrika* **30**, 81–89 (1938).
38. Amaral, L. A. N., Scala, A., Barthelemy, M. & Stanley, H. E. Classes of small-world networks. *PNAS* **97**, 11149–11152 (2000).
39. Yan, X. Y., Zhou, T. & Destination Choice Game: A Spatial Interaction Theory on Human Mobility. *Natural Resources* **2**, 234–239 (2018).
40. Klemm, K., Serrano, M. Á., Eguíluz, V. M. & San Miguel, M. A measure of individual role in collective dynamics. *Sci. Rep.* **2**, 292 (2012).
41. Liu, J. G., Lin, J. H., Guo, Q. & Zhou, T. Locating influential nodes via dynamics-sensitive centrality. *Sci. Rep.* **6**, 21380 (2016).
42. Yan, G., Fu, Z. Q. & Chen, G. Epidemic threshold and phase transition in scale-free networks with asymmetric infection. *Eur. Phys. J. B* **65**, 591–594 (2008).
43. Wang, W. *et al.* Asymmetrically interacting spreading dynamics on complex layered networks. *Sci. Rep.* **4**, 5097 (2014).
44. Hirsch, J. E. An index to quantify an individual's scientific research output. *Proc. Natl. Acad. Sci. USA* **102**, 16569–16572 (2005).

Acknowledgements

The authors acknowledge DataCastle to hold the related world-wide competition and to share the data. This work is partially supported by National Natural Science Foundation of China (61473073, 61104074, 61433014), Fundamental Research Funds for the Central Universities (N161702001, N171706003), and Program for Liaoning Excellent Talents in University (LJQ2014028).

Author Contributions

Z.L., T.R. and T.Z. devised the research project. S.M.L. and Y.X.Z. performed the research. Z.L., T.R., S.M.L., Y.X.Z. and T.Z. analyzed the data. Z.L., T.R., X.Q.M., S.M.L., Y.X.Z. and T.Z. wrote the paper.

Additional Information

Competing Interests: The authors declare no competing interests.

Publisher's note: Springer Nature remains neutral with regard to jurisdictional claims in published maps and institutional affiliations.



Open Access This article is licensed under a Creative Commons Attribution 4.0 International License, which permits use, sharing, adaptation, distribution and reproduction in any medium or format, as long as you give appropriate credit to the original author(s) and the source, provide a link to the Creative Commons license, and indicate if changes were made. The images or other third party material in this article are included in the article's Creative Commons license, unless indicated otherwise in a credit line to the material. If material is not included in the article's Creative Commons license and your intended use is not permitted by statutory regulation or exceeds the permitted use, you will need to obtain permission directly from the copyright holder. To view a copy of this license, visit <http://creativecommons.org/licenses/by/4.0/>.

© The Author(s) 2019